VU Research Portal

High-density surface electromyography improves the identification of oscillatory synaptic inputs to motor neurons

van de Steeg, C.; Daffertshofer, A.; Stegeman, D.F.; Boonstra, T.W.

Link to publication in VU Research Portal

High-density surface electromyography improves the identification of oscillatory synaptic inputs to motoneurons

Chiel van de Steeg, Andreas Daffertshofer, Dick F. Stegeman and Tjeerd W. Boonstra

High-density surface electromyography improves the identification of oscillatory synaptic inputs to motoneurons

Chiel van de Steeg,[1] **Andreas Daffertshofer,**[1] **Dick F. Stegeman,**[1,2] **and Tjeerd W. Boonstra**[1,3,4]

[1]*MOVE Research Institute, Vrije Universiteit Amsterdam, Amsterdam, The Netherlands;* [2]*Donders Institute for Brain, Cognition and Behavior, Radboud University, Nijmegen Medical Centre, Nijmegen, The Netherlands;* [3]*School of Psychiatry, University of New South Wales, Sydney, Australia; and* [4]*Black Dog Institute, Sydney, Australia*

van de Steeg C, Daffertshofer A, Stegeman DF, Boonstra TW. High-density surface electromyography improves the identification of oscillatory synaptic inputs to motoneurons. *J Appl Physiol* 116: 1263–1271, 2014. First published March 20, 2014; doi:10.1152/japplphysiol.01092.2013.— Many studies have addressed corticomuscular coherence (CMC), but broad applications are limited by low coherence values and the variability across subjects and recordings. Here, we investigated how the use of high-density surface electromyography (HDsEMG) can improve the detection of CMC. Sixteen healthy subjects performed isometric contractions at six low-force levels using a pinch-grip, while HDsEMG of the adductor pollicis transversus and flexor and abductor pollicis brevis and whole-head magnetoencephalography were recorded. Different configurations were constructed from the HDsEMG grid, such as a bipolar and Laplacian montage, as well as a montage based on principal component analysis (PCA). CMC was estimated for each configuration, and the strength of coherence was compared across configurations. As expected, performance of the precision-grip task resulted in significant CMC in the β-frequency band (16–26 Hz). Compared with a bipolar EMG montage, all multichannel configurations obtained from the HDsEMG grid revealed a significant increase in CMC. The configuration, based on PCA, showed the largest (37%) increase. HDsEMG did not reduce the between-subject variability; rather, many configurations showed an increased coefficient of variation. Increased CMC presumably reflects the ability of HDsEMG to counteract inherent EMG signal factors—such as amplitude cancellation—which impact the detection of oscillatory inputs. In contrast, the between-subject variability of CMC most likely has a cortical origin.

corticomuscular coherence; common oscillatory drive; surface EMG; motor unit; amplitude cancellation

FUNCTIONAL CONNECTIVITY ANALYSIS is widely used to investigate descending drive to muscles. Corticomuscular coherence (CMC), between the electromyogram (EMG) of a contracting muscle and electroencephalographic (EEG) or magnetoencephalographic (MEG) recordings over the contralateral primary cortex, has been found predominantly in the β band (15–30 Hz) during precision grip. It reflects synchronized oscillatory discharge of pyramidal cells projecting to the spinal cord (1, 10, 34, 47). CMC in the β band is present mainly during tonic muscle contractions and is hence considered important for stabilizing current motor output (9, 14, 23, 37, 56). Intermuscular coherence between EMG of two contracting muscles has been reported in both β- and α-frequency (8–12 Hz) ranges and represents synchronized oscillatory input to different muscles (7, 12, 15, 20, 24). Estimation of both corticomuscular and intermuscular coherence typically relies on surface EMG recordings. The capacity of surface EMG to identify oscillatory synaptic inputs to motoneurons is therefore crucial (16, 17).

Coherence analysis may advance our understanding of the pathogenesis of movement disorders (40, 48). It has been used to investigate mechanisms underlying cocontraction in dystonia (22), the origin of essential and orthostatic tremor (27, 35, 41), Parkinsonian resting tremor (54), abnormal corticomuscular interactions in X-linked Kallmann syndrome (21), adaptations following wrist and hand immobilization (36), and changes in CMC with age (30). Despite abundant examples of abnormalities in long-range synchronization, reported CMC is generally low, which questions its functional relevance and reduces the statistical power to detect pathological changes. Moreover, between-subject variability is typically high, and a considerable percentage of healthy subjects does not show any significant CMC (8, 39, 46). To increase clinical applicability and its potential diagnostic value, a first goal should be improved reliability of corticomuscular and intermuscular coherence.

Coherence provides an indirect measure of the interactions between the neurophysiological processes that are measured. Whereas the motor-unit pool has a seemingly linear transfer function, which enables the transmission of oscillatory components in the presynaptic drive to the muscles (43, 52), several factors may affect the way these components are translated in surface EMG recordings (4, 19). For instance, placement of the electrodes close to or over the endplate strongly comprises the detection of common oscillatory components in surface EMG (33). In addition, amplitude cancellation strongly affects surface EMG recordings (32) and also impacts the detection of common oscillatory input to the motoneurons (19). Similarly, EEG and MEG signals are generally thought to result from dendritic currents in pyramidal cells (25) and hence, only have an indirect relationship to the discharge patterns of pyramidal cells. Volume conduction and the limited spatial resolution of these recording techniques hamper the detection and isolation of activity from pyramidal cells that innervate a particular muscle of interest (45).

Although signal acquisition and analysis problems can be identified at a central and a peripheral level, we focused here on the latter, thus on factors that affect the transmission of oscillatory activity into surface EMG recordings and impede the assessment of CMC. We tested the ability of high-density surface EMG (HDsEMG) to optimize the quality of the often-overlooked peripheral side and to obtain a more reliable estimate of the oscillatory synaptic inputs to motoneurons. HDsEMG has been used to improve the prediction of the force that is generated with a particular muscle (50). We use HDsEMG

Address for reprint requests and other correspondence: T. W. Boonstra, School of Psychiatry, Black Dog Institute Bldg., Hospital Rd., Randwick, NSW 2031, Australia (e-mail: t.boonstra@unsw.edu.au).

instead to assess the presynaptic input to the motor-unit pool. HDsEMG can easily overcome potential problems with the correct electrode placement (33) and is also thought to reduce the impact of amplitude cancellation (51). We recorded whole-head MEG and HDsEMG of intrinsic hand muscles while subjects performed a simple pinch-grip task. Different electrode configurations were constructed offline from the electrode grid, and CMC was compared across configurations. We expected that HDsEMG would improve the identification of oscillatory synaptic inputs reflected by increased CMC. If the variability between subjects is determined by peripheral factors, HDsEMG should also reduce the between-subject variability of CMC. Such improvements will increase the clinical potential of CMC.

MATERIALS AND METHODS

Subjects

Sixteen healthy subjects (nine women, age $\pm$ SD = 31.6 $\pm$ 7.6 yr) volunteered in the study. The Local Ethics Committee at the Faculty of Human Movement Sciences, Vrije Universiteit Amsterdam, approved the experimental protocol, and before recordings, each subject provided written, informed consent. The experiments were conducted in accordance with the Declaration of Helsinki.

Experimental Protocol

Subjects were instructed to generate prescribed force levels using a pinch grip while lying supine in the MEG scanner. Visual feedback of the generated force and the target force was projected on the ceiling. Subjects generated force by squeezing a sensor (Fig. 1A) between their right thumb and index finger, and target force levels were set at 0 (just holding), 0.6, 0.95, 1.3, 1.65, and 2 N, respectively. Each force level had to be maintained for 30 s. Subjects had a 12-s break between subsequent trials. Before recording, subjects were acquainted with the setup and trained to control the display comfortably.

Data Acquisition

CMC was assessed using MEG and HDsEMG. EMG was recorded using a 64-channel HDsEMG (8×8; interelectrode distance, 4 mm; Fig. 1B) electrode grid with a 128-channel Refa amplifier (sampling rate, 1,024 Hz; TMSi, Enschede, The Netherlands;). The grid was placed over the mm. adductor pollicis transversus and flexor and abductor pollicis brevis (Fig. 1C). MEG (306 channels), ECG, electrooculography, and head position were recorded using a Vectorview Neuromag system (sampling rate, 1,250 Hz; Elekta, Stockholm, Sweden). Grip force was recorded simultaneously using a custom-made MEG-compatible force sensor (5, 55) (Fig. 1A). Recordings were synchronized offline using a 2-Hz analog transistor–transistor logic (TTL) pulse sent from the MEG to the EMG amplifier. The TTL pulse was recorded at one EMG channel, leaving 63 EMG channels for further analysis.

Preprocessing

MEG signals were first transformed to standard head position and filtered for spatiotemporal signal-space separation (53). Further offline processing was realized in Matlab (2011b; MathWorks, Natick, MA). HDsEMG was linearly interpolated to 1,250 Hz and synchronized to MEG via the aforementioned TTL pulse.

The HDsEMG signals were rereferenced to the most proximal-lateral electrode of the electrode grid (closest to the thumb) and high-pass filtered using a bidirectional third-order Butterworth filter (cutoff frequency, 10 Hz). The first 2 s of every trial were discarded to avoid transient motor behavior.
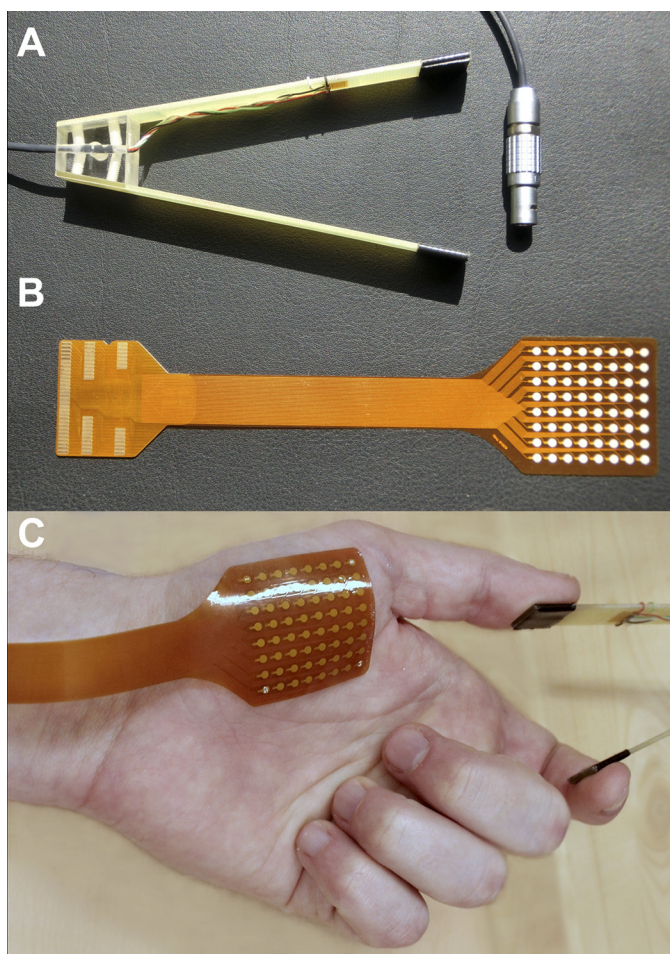

Fig. 1. Force transducer and high-density surface electromyography (HDsEMG) electrode grid. *A*: magnetoencephalographic (MEG)-compatible force sensor, custom-made for pinch-grip recordings. *B*: 64-channel (8 × 8) electrode grid. *C*: electrode grid placed over parts of the mm. adductor pollicis transversus and flexor and abductor pollicis brevis.

Data Analysis

Next, we determined the power-spectral density and magnitude-squared coherence between MEG and HDsEMG. Power and coherence were estimated using Welch's periodogram method with a unit-energy Hamming window of 500 ms and 50% overlap. The 95% confidence interval was determined using sets of surrogate data of linear-independent signals (6, 29). By randomizing the Fourier phases of the MEG and EMG signals, 100 surrogates were generated from each subject (31). Subsequently, coherence was computed between the surrogate sets, identical to the original data, and the 95% confidence intervals were determined. These intervals were used to determine the frequency band with significant coherence on group level. Both the peak values and the average CMC of this frequency band were compared across EMG configurations.

We first computed the coherence between all available channels, yielding a 306 × 63 coherence matrix. Since the focus of this study is on effects of high-density assessment of the EMG, we selected the MEG channel that displayed maximal coherence values in the frequency band (16–26 Hz) and used this channel and its seven nearest neighbors for further analysis. As expected, these MEG channels were located above the left (contralateral) sensorimotor cortex.

EMG configurations. EMG data were collected via a 64-channel electrode grid (Fig. 1B), using average reference. From this set, distinct electrode configurations were constructed (Fig. 2). Multiple
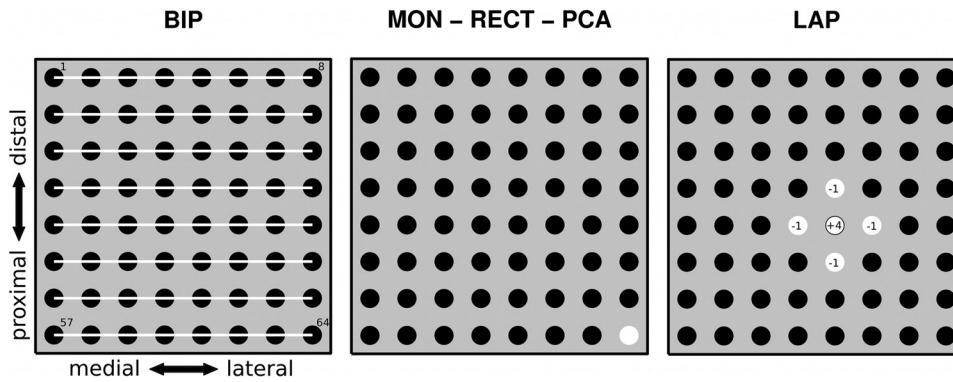
Fig. 2. Configurations derived from the HD-sEMG electrode grid. Results of 5 different EMG procedures: bipolar configuration (BIP), nonrectified/rectified monopolar set (MON/RECT), principal component analysis (PCA; eigenvalue threshold), and Laplacian configuration (LAP). MON, RECT, and PCA configurations are rereferenced to the most proximal-lateral electrode (*middle*). All configurations are derived for all available electrodes on the entire grid.

bipolar electrode configurations were constructed over the entire grid using closest-neighboring electrode pairs in the medial-lateral direction, approximately corresponding to the direction of the muscle fibers. The bipolar configuration (BIP) was used as a reference to allow the comparison with the conventional approach for assessing CMC. Multiple monopolar montages were constructed by rereferencing the EMG signals against the most proximal-lateral electrode of the electrode grid (closest to the thumb; Fig. 2, *middle*). Rereference montages are indicated by a "r" at the end of the acronym, e.g., "MONr". For this monopolar montage, both the nonrectified (MONr) and rectified (RECTr) EMG were considered. A higher-order spatial filtering, Laplacian configuration, was constructed for all available electrodes over the entire grid, having a central electrode weighted with a factor of four and four closest-neighboring electrodes weighted with a factor of −1 (Fig. 2, *right*).

Each EMG configuration was derived for all available electrodes on the entire grid and would hence result in multiple CMC spectra. To obtain a single coherence spectrum for each configuration, we followed two approaches: *1*) the constructed EMG signals were averaged before computing the coherence with each of the eight preselected MEG channels and averaged over the resulting eight coherence values, or *2*) coherence was computed between each constructed EMG signal and each of the eight MEG channels and averaged across all channel combinations. Configurations, for which the EMG signals were averaged before computing coherence, are indicated by a "m" at the beginning of the acronym, e.g., "mBIP". Table 1 outlines the 12

Table 1. *Overview of EMG configurations*

Configuration	Rereferenced	Rectified	Derivative	Averaged*
BIP	No	Yes	Bipolar	MSC
LAP	No	Yes	Laplacian	MSC
MONr	Yes	No		MSC
RECTr	Yes	Yes		MSC
PCA	No	Yes	PCA	MSC
PCAr	Yes	Yes	PCA	MSC
mBIP	No	Yes	Bipolar	HDsEMG
mMONr	Yes	No		HDsEMG
mRECTr	Yes	Yes		HDsEMG
mLAP	No	Yes	Laplacian	HDsEMG
mPCA	No	Yes	PCA	HDsEMG
mPCAr	Yes	Yes	PCA	HDsEMG

*Magnitude-squared coherence (MSC), corticomuscular coherence (CMC) is first computed for each electrode of the high-density surface electromyography (HDsEMG) configuration, and then coherence is averaged across electrodes. HDsEMG, EMG signals are first averaged across all electrodes of the HDsEMG configuration, and then CMC is computed between the average EMG signal and MEG. BIP, bipolar configuration; LAP, Laplacian configuration; MON, nonrectified; r, rereference montages; RECT, rectified; PCA, principal component analysis; m, EMG signals averaged before computing coherence.

configurations that we tested and the preprocessing steps that were involved.

Principal component analysis. We decomposed all HDsEMG signals of the electrode grid into principal components. Principal component analysis (PCA) is a well-established method to capture redundant information in multidimensional data sets by means of mode reduction (11). Previous studies have shown that removing the leading principal components one by one improves the estimation of muscle force from EMG recordings (50, 51). This method can be seen as a data-driven filter; that is, the leading components capture the correlated patterns that account for as much of the variability in the data as possible. The patterns that are common across all channels of the electrode grid appear to add little information about muscle force, because after removal of these modes, the force estimation improves. Here, we adopted that approach to test whether removing the leading modes may also improve the detection of oscillatory synaptic inputs to motoneurons and hence may increase CMC. The leading components were removed one by one and the resulting EMG signals rectified before computing coherence. The number of to-be-removed principal components was determined by optimizing the resulting coherence, averaged over the eight MEG channels.

Statistical Analysis

The mean coherence value of each EMG configuration was normalized to the coherence value corresponding to the conventional BIP and expressed as percentage change to minimize the between-subject variability. To assess whether a configuration revealed a significant increase in coherence, these percentages were compared against zero using a one-sample *t*-test.

Between-subject variability was quantified by the coefficient of variation (CV), i.e., dividing the group mean by the SD. Because the CV is defined at group level rather than for each subject individually, the SD of this outcome measure had to be determined using a bootstrapping approach (13). The SD was determined using 1,000 bootstrap samples. To test for significant changes in between-subject variability, the CV of each configuration was compared against the BIP configuration using a paired two-sample *t*-test.

For both analyses, the significance threshold of 0.05 was adjusted for multiple comparisons using Bonferroni correction.

RESULTS

We compared CMC in the β band during precision grip in 12 configurations derived from HDsEMG (Table 1) to test its ability for improving coherence estimates. We first computed the power-spectral densities to investigate the spectral peaks present in the EMG signals and to compare them across configurations. Figure 3 shows the grand-average power spectral densities for all 12 configurations. Spectra for configurations based on nonrectified EMG (MONr and mMONr) differed considerably from the other configurations, based on
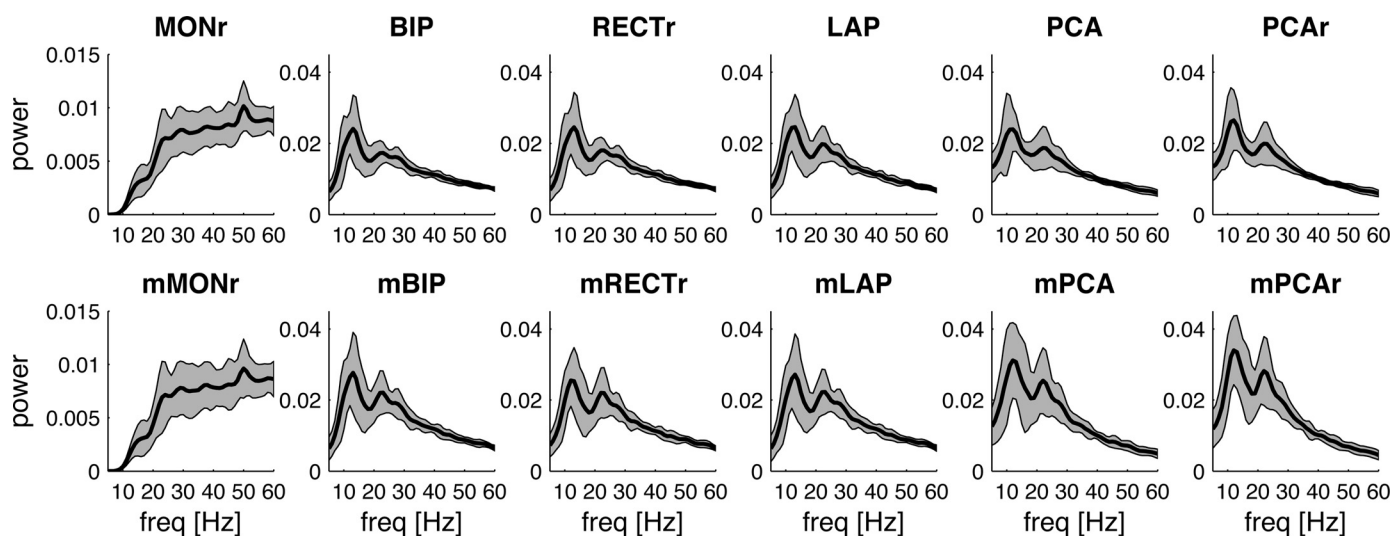
Fig. 3. Grand-average power-spectral densities showing EMG for the 12 configurations' power at a force level of 2 N. Black lines show the average; gray patches depict the standard deviation across subjects. Spectra are normalized to total power. r, rereference montages; m, EMG signals averaged before computing coherence.

rectified EMG: whereas nonrectified EMG mainly revealed power at higher frequencies (>20 Hz), rectification resulted in a shift of power toward lower frequencies. Configurations based on rectified coherence all showed a pronounced peak, approximately 10–15 Hz, which reflects the average firing rate of the motoneurons (42). In addition, most configurations revealed a second peak, approximately 20–25 Hz. The strength of these peaks varied across configurations and was generally larger in configurations in which signals were averaged across the electrode grid before computing power and coherence (Fig. 3, *bottom*). In particular, configurations based on PCA revealed a large peak at 10–15 and 20–25 Hz (mPCA and mPCAr).

In accordance with the literature, we found significant CMC in the β band. CMC was strongest for MEG channels over

the contralateral sensorimotor cortex, although there was some variability in the exact location of the maximum across subjects (Fig. 4). In addition, large differences in the magnitude of CMC were observed across subjects: whereas some subjects showed pronounced coherence levels [e.g., >0.15 in S16], other subjects revealed no significant CMC (e.g., S1, S4, S11). We used the eight channels showing maximal CMC in the grand-average topology for further statistical analysis and averaged CMC across these eight channels. The location of these MEG channels is shown in Fig. 4.

Figure 5 shows the grand-average coherence spectra for two configurations for the six force levels that we tested. We used the BIP to determine the frequency band showing significant

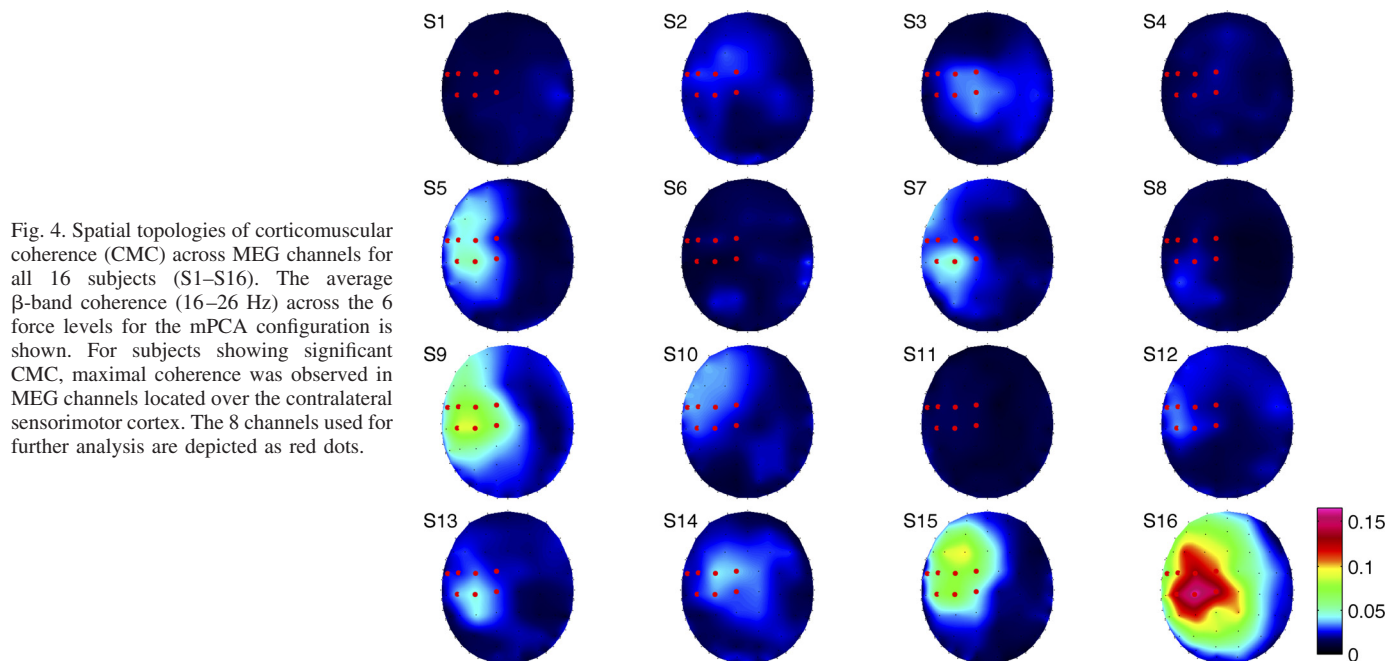Fig. 4. Spatial topologies of corticomuscular coherence (CMC) across MEG channels for all 16 subjects (S1–S16). The average β-band coherence (16–26 Hz) across the 6 force levels for the mPCA configuration is shown. For subjects showing significant CMC, maximal coherence was observed in MEG channels located over the contralateral sensorimotor cortex. The 8 channels used for further analysis are depicted as red dots.
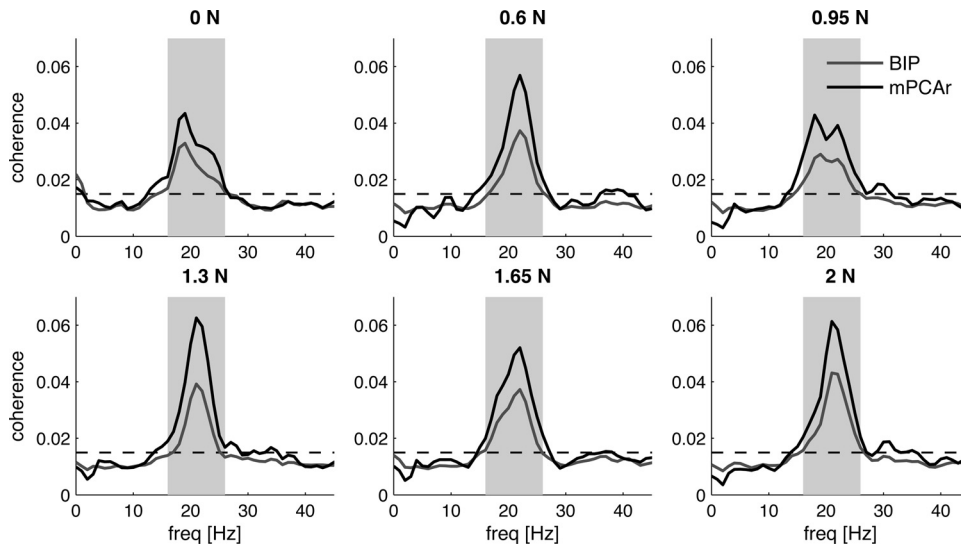
Fig. 5. Grand-average coherence spectra showing CMC at 6 force levels (0, 0.6, 0.95, 1.3, 1.65, and 2 N) for 2 EMG configurations (BIP, gray lines; mPCAr, black lines). Dashed lines show the 95% confidence interval obtained via phase randomization. Gray patches depict the frequency band that showed significant coherence on a group level for the BIP, i.e., 16–26 Hz. Both EMG configurations show significant coherence at the same frequencies, but coherence is elevated for the mPCAr configuration for all force levels.

coherence: on the 16- to 26-Hz frequency interval, the group average exceeded the 95% confidence interval. The configuration based on PCA (mPCAr) revealed increased coherence in the same frequency range but little change at other frequencies. PCA can be seen as a data-driven filter, and the number of to-be-removed principal components was determined via optimizing the resulting coherence estimate separately for each subject. On average, we removed the leading seven principal components (PCA 3.8 ± 3.2, PCAr 7.1 ± 4.5, mPCA 8.6 ± 3.6, and mPCAr 9.1 ± 3.6).

Because we did not find a significant difference in CMC across force levels, we pooled coherence across trials to obtain a better signal-to-noise ratio of the coherence estimate. Compared against the bipolar montage as a reference, the other 11 HDsEMG configurations showed a significant increase in β-band coherence. Table 2 summarizes the results for all configurations. The configuration based on PCA (mPCA and mPCAr) revealed the largest increase in mean CMC, i.e., 37%. This configuration corresponds to the approach described by Staudenmann et al. (50).

CMC varied considerably across subjects. Figure 6 shows the coherence spectra for all 16 subjects for two configurations (BIP and mPCAr). Again, both configurations showed significant coherence in the same frequency ranges, and the mPCAr configuration showed increased coherence in all subjects showing significant coherence. Of the 16 subjects, nine showed significant coherence (peak coherence in the 16- to 26-Hz frequency interval exceeded the 95% confidence interval) when estimated using a bipolar montage (BIP). This increased to 12 out of 16 subjects for the mPCAr configuration. Although these HDsEMG configurations revealed an increased number of subjects with significant coherence, the increase in coherence for these configurations was mainly confined to the subjects who already showed significant coherence. In the subjects showing little or no β-band coherence (S1, S4, S6, S10, and S11), the increase in coherence for the mPCAr configuration is negligible (see Fig. 6).

The CV for all configurations was considerably high (~0.3) and showed an increase compared with the BIP (Fig. 7B). That increase, however, was only significant in four configurations

Table 2. *CMC for different EMG configurations*

Configuration	Peak CMC		Mean CMC			% Change			CV		
	Mean	SE	Mean	SE	# Sign.	Mean	SE	P	Mean	SE	P
BIP	0.040	0.010	0.025	0.005	9				0.27	0.010	
MONr	0.049	0.014	0.030	0.008	9	15.34	3.38	0.0005*	0.29	0.008	0.71
RECTr	0.047	0.011	0.029	0.006	11	15.69	3.93	0.0015*	0.31	0.011	0.0012*
LAP	0.043	0.011	0.026	0.006	9	5.78	1.59	0.0031*	0.27	0.011	0.56
PCA	0.045	0.011	0.028	0.006	10	13.04	2.81	0.0004*	0.29	0.011	0.072
PCAr	0.047	0.011	0.029	0.006	11	17.22	3.60	0.0003*	0.30	0.010	0.0048
mBIP	0.052	0.013	0.031	0.007	11	20.93	4.71	0.0006*	0.29	0.011	0.024
mMONr	0.055	0.015	0.033	0.008	11	28.76	5.66	0.0002*	0.29	0.011	0.022
mRECTr	0.051	0.012	0.031	0.007	11	23.79	6.64	0.0034*	0.32	0.011	0.0002*
mLAP	0.052	0.012	0.030	0.007	11	22.54	5.02	0.0006*	0.29	0.011	0.055
mPCA	0.058	0.014	0.035	0.008	12	37.41	5.43	0.0000*	0.31	0.010	0.0006*
mPCAr	0.057	0.014	0.035	0.008	12	37.31	5.63	0.0000*	0.32	0.010	0.0002*

*Statistically significant after Bonferroni correction ($P < 0.0045$). Both peak CMC and mean coherence in the frequency range from 16 to 26 Hz were compared. The number of subjects showing significant CMC (# Sign.) was determined by whether peak CMC exceeded the 95% confidence interval. The increase in mean CMC (% Change) was determined against the BIP, and the significance of this increase (P) was determined using a 1-sample t-test. The coefficient of variation (CV) was defined as the SD across subjects, divided by the mean. Again, significant changes against the BIP configuration were determined using a t-test.
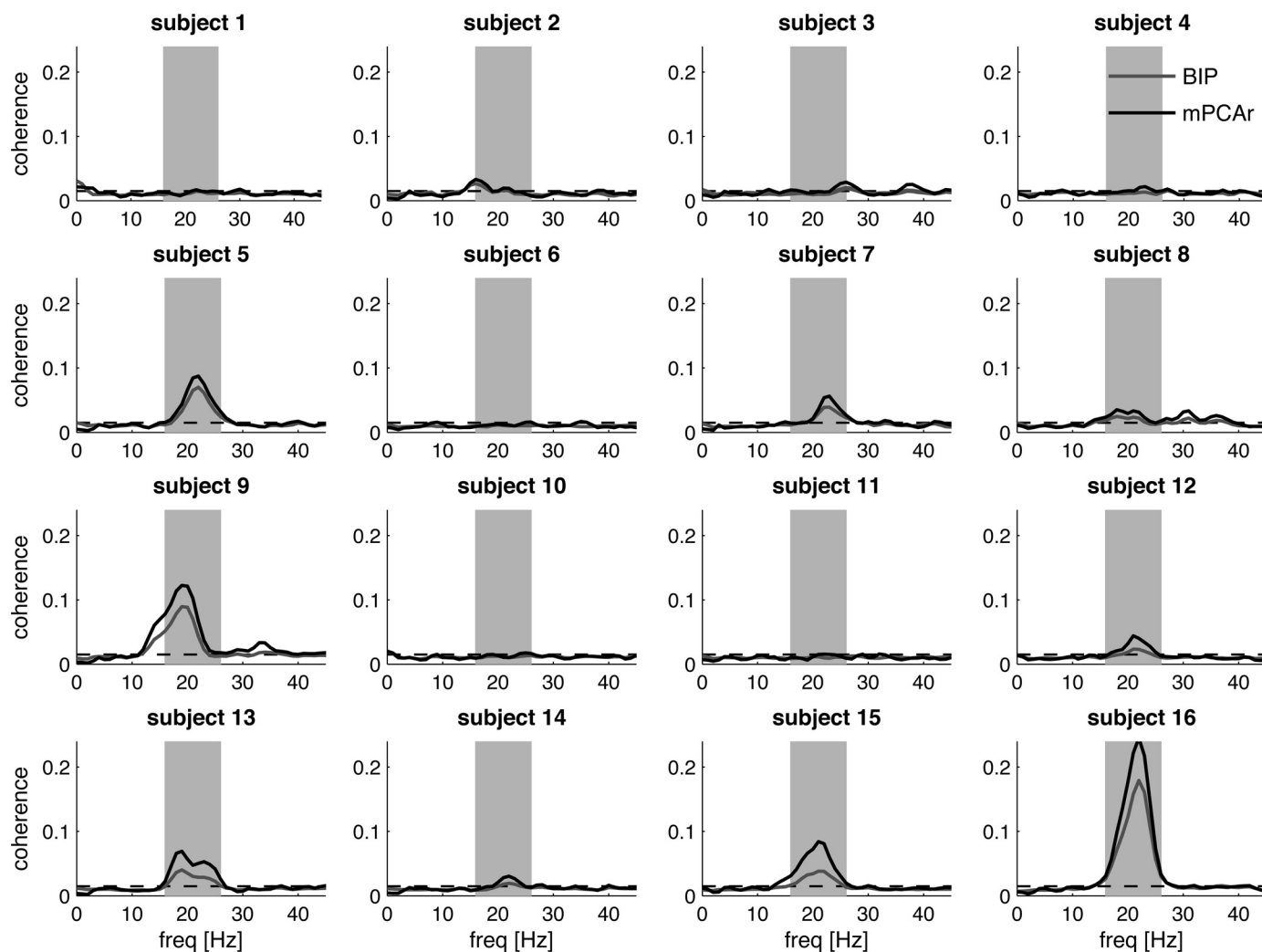
Fig. 6. CMC for all 16 subjects obtained from 2 different HDsEMG configurations (BIP, gray lines; mPCAr, black lines). Dashed lines show the 95% confidence interval obtained via phase randomization. Gray patches depict the frequency band that shows significant coherence on a group level (16–26 Hz). In all subjects showing significant coherence in the β band, the mPCAr configuration shows higher coherence levels than the BIP configuration.

(RECTr, mRECTr, mPCA, and mPCAr; see Table 2). When comparing the increases in CV with the increase in coherence (Fig. 7*A*), they both reveal a similar pattern. This confirms that the increase in coherence for HDsEMG configurations was largely confined to the subjects who already showed significant coherence rather than uncovering CMC in subjects who did not show significant coherence in the bipolar montage.

DISCUSSION

This study investigated how the estimation of CMC can be improved by using HDsEMG. Whole-head MEG and 64-channel HDsEMG of the adductor pollicis transversus and flexor and abductor pollicis brevis were recorded while subjects performed a precision-grip task. In agreement with previous studies, we found significant CMC in the β-frequency band (16–26 Hz). The strength of β-band coherence was compared across 11 EMG configurations derived from the HDsEMG grid, with the conventional bipolar montage as a reference. All configurations showed a significant increase in CMC against a bipolar montage after correcting for multiple comparisons. The CV revealed considerable variability be-

tween subjects (~30%). Compared with the bipolar montage, the CV increased for all EMG configurations, although the increase was only significant in four configurations after correcting for multiple comparisons. The largest increase in coherence was found for configurations derived by PCA, as described by Staudenmann et al. (50), showing a 37% increase, on average (range: approximately 10–100%), compared with bipolar EMG. Hence, HDsEMG improves the detection of oscillatory synaptic inputs—mainly in subjects who already showed significant coherence—but does not reduce the between-subject variability in CMC.

The 37% increase in CMC, obtained by processing HDsEMG with PCA, closely matches the 40% improvement in force estimation using the same method (50). Staudenmann et al. (50, 51) conclude that HDsEMG improves EMG amplitude estimation by reducing effects of so-called far-field activity, amplitude cancellation, and adequate representation of the heterogeneous activity of motor units within a muscle. Simulation studies have shown that heterogeneity and amplitude cancellation also negatively impact the estimation of cortico-muscular and intermuscular coherence (4, 19). Hence, the
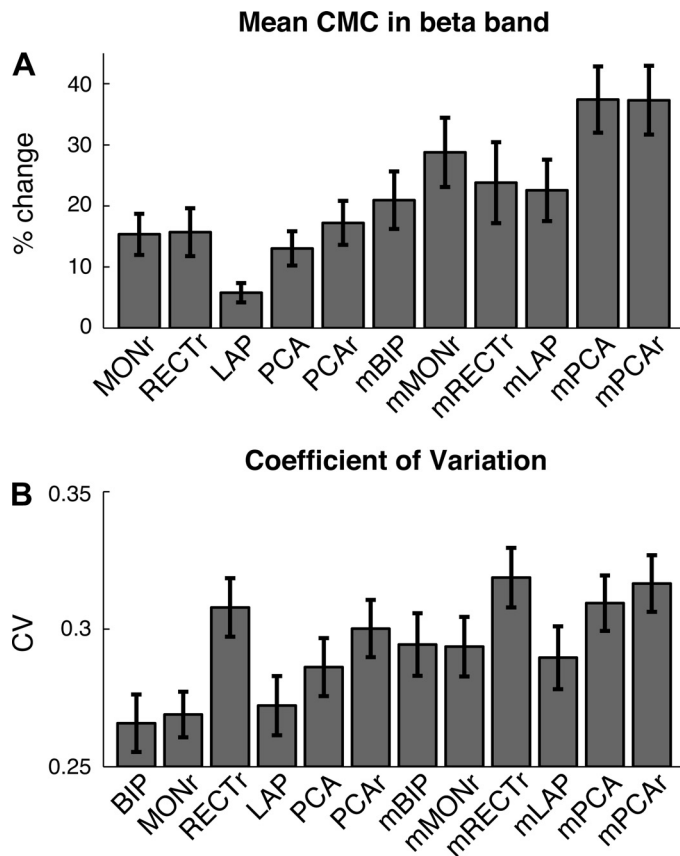
A Mean CMC in beta band

B Coefficient of Variation

Fig. 7. Group results of CMC in the β band. *A*: mean coherence in the 16- to 26-Hz frequency band for the different EMG configurations. Coherence values are expressed as percentage change against our reference BIP. Error bars depict the SE. *B*: coefficient of variation (CV) of CMC in the β band, showing the between-subject variability for different EMG configurations. Error bars depict the SE. For the CV, SE is estimated using a bootstrapping approach.

almost-identical improvement in CMC found in the present study and improvement in force estimation reported in literature most likely reflect the same underlying mechanisms, in keeping with a linear transfer function of the motor-unit pool (18, 52). That is, methods that improve force estimation or the output of the motor-unit pool are also likely to improve the estimation of oscillatory components in the input to the motoneurons. Amplitude cancellation, caused by overlapping positive and negative phases of motor-unit potentials, strongly impacts on surface EMG recordings (32). The reduction of the effect of factors, such as amplitude cancellation, would have important consequences for the interpretation of corticomuscular and intermuscular coherence (28), allowing better comparison between conditions that are known to affect amplitude cancellation, such as muscle fatigue (49).

The PCA approach can be compared with other preprocessing methods (e.g., rectification, whitening, or high-pass filtering) that affect the temporal characteristics of the EMG signal. In particular, the use of rectification of surface EMG to improve the identification of oscillatory synaptic inputs in corticomuscular and intermuscular coherence has been heavily debated (4, 19, 38, 42, 44, 52, 57, 61). The efficacy of rectification depends on a number of factors, such as the heterogeneity in the motor-unit action potentials (4) and the number of active motor units and their firing rates (19), and

may hence vary across conditions. It has been suggested that the extent to which raw and rectified EMG reflects the spectrum of common input to motoneurons depends on amplitude cancellation and that EMG rectification is preferable when contraction strengths are low (19). Experimental data indeed support that at low contraction levels (0.05 and 0.4 N), rectified EMG is a better predictor of oscillatory components in motoneuron spiking data (57). In the present study, which is at similar low contraction levels (0–2 N), both RECTr and MONr EMG resulted in an increase of ~15% compared with bipolar EMG (see Fig. 7). In contrast to Ward et al. (57), who recorded EMG from the extensor digitorum longus muscle, we recorded HDsEMG from the adductor pollicis transversus and flexor and abductor pollicis brevis, demonstrating that the effect of rectification is dependent on the muscle architecture (4). What is important to note is that the increase in CMC for RECTr and MONr was much smaller than the 37% increase for the PCA method (mPCA and mPCAr). High-pass filtering, at very high cutoff frequencies before rectification, has also been proposed as a tool to improve coherence analysis (4). Here, we did not observe increased CMC after high-pass filtering at frequencies >10 Hz (results not shown). Together, these findings suggest that the spatial information captured by HDsEMG yields additional information about the oscillatory synaptic inputs compared with methods that only capitalize on the temporal characteristics of EMG and hence, demonstrate the use of HDsEMG in coherence analysis. Indeed, all configurations, in which EMG signals are averaged across all electrodes of the HDsEMG before computing coherence (indicated by m at the beginning of the acronym), revealed the largest increase in CMC in the β band (Fig. 7).

HDsEMG did not reduce the between-subject variability of CMC. In fact, four HDsEMG configurations showed a significant increase in CV compared with the bipolar montage. The results show that HDsEMG mainly increases coherence in subjects who already showed significant coherence. It is therefore unlikely that the large variability between subjects is caused by peripheral factors, such as incorrect placement of EMG electrodes (33). Potential sources of variability are the capacity to record the corticospinal drive using encephalographic methods, such as EEG and MEG, the composition of the corticospinal drive itself, and spinal mechanisms that affect the transmission of the corticospinal drive to the motoneurons. EEG and MEG are indirect measures reflecting dendritic currents in pyramidal cells, and the number of simultaneously active cortical neurons is a number of magnitudes larger than the number of active motoneurons. The resulting amplitude cancellation is therefore so pervasive that the measured signals can only be generated by synchronized neuronal activity of large numbers of neurons (25). In the present study, we deliberately minimized MEG processing to focus on effects of the periphery, but spatial configurations, such as a Laplacian montage, may also be used to improve the signal-to-noise ratio in EEG and MEG (45). In fact, MEG-source reconstruction techniques have been used to improve coherence estimates (2).

Rather than a measurement problem, the variability may reflect inherent properties of the corticospinal drive. In most computational studies, it is assumed that the corticospinal drive is spatially homogenous. However, the activity of numerous pyramidal neurons projecting onto the same motoneuron may not be fully synchronized. Spatial inhomogeneity strongly

reduces oscillatory components in the net drive and thereby also reduces CMC (26). Variability between subjects may thus reflect the degree of synchronization between pyramidal neurons projecting to the same muscle. Spinal mechanisms may also prevent the transmission of oscillatory components to the motoneuron pool. For instance, Williams and Baker (58) and Williams et al. (59) have proposed a spinal circuitry that acts as a filter to suppress oscillatory components in the corticospinal drive. Interestingly, a recent study showed significant CMC in all subjects in a study on motor adaptation (39). Subjects had to produce isometric force against a manipulandum and had to compensate for mechanical force perturbations to their finger. Whereas eight out of 14 subjects showed significant CMC at the beginning of the experiment, the other six subjects only showed significant CMC after learning the dynamic force task. These results underscore the role of afferent feedback in CMC and the possibility that individual differences in the occurrence of CMC can be changed with learning. β-Band coherence is thought to be involved in sensorimotor integration (60), and the absence of CMC may hence reflect differences in task execution.

In summary, HDsEMG can improve the identification of oscillatory synaptic inputs to motoneurons. A configuration based on PCA resulted in a 37% increase in CMC in the β band. This increase reflects the ability of HDsEMG to minimize factors that impact the identification of common oscillatory input from surface EMG recordings, such as far-field activity, amplitude cancellation, and the heterogeneity of motoneurons. The reduction of the influence of these EMG-related factors on the coherence estimate facilitates the comparison of CMC between conditions in which these factors are changed (3). Moreover, higher coherence values increase the statistical power to differentiate between conditions. Hence, the use of HDsEMG may help to improve the clinical application of CMC. However, the large variability in CMC between healthy subjects is the major drawback for such clinical applications. That is, the absence of significant CMC in healthy controls hampers the use of CMC as a diagnostic tool for deficiencies in the corticospinal tract. Further research is required to identify the nature of this variability and its functional relevance in motor control.

GRANTS

DISCLOSURES

The authors have no conflicts of interest.

AUTHOR CONTRIBUTIONS

Author contributions: C.v.d.S., A.D., D.S., and T.W.B. conception and design of research; C.v.d.S. performed experiments; C.v.d.S., A.D., and T.W.B. analyzed data; C.v.d.S., A.D., D.S., and T.W.B. interpreted results of experiments; C.v.d.S. and T.W.B. prepared figures; C.v.d.S., A.D., and T.W.B. drafted manuscript; C.v.d.S., A.D., D.S., and T.W.B. edited and revised manuscript; C.v.d.S., A.D., D.S., and T.W.B. approved final version of manuscript.

REFERENCES

1. **Baker SN, Olivier E, Lemon RN.** Coherent oscillations in monkey motor cortex and hand muscle EMG show task-dependent modulation. *J Physiol* 501: 225–241, 1997.

2. **Bayraktaroglu Z, von Carlowitz-Ghori K, Losch F, Nolte G, Curio G, Nikulin VV.** Optimal imaging of cortico-muscular coherence through a novel regression technique based on multi-channel EEG and un-rectified EMG. *Neuroimage* 57: 1059–1067, 2011.

3. **Boonstra TW.** The potential of corticomuscular and intermuscular coherence for research on human motor control. *Front Hum Neurosci* 7: 855, 2013.

4. **Boonstra TW, Breakspear M.** Neural mechanisms of intermuscular coherence: implications for the rectification of surface electromyography. *J Neurophysiol* 107: 796–807, 2012.

5. **Boonstra TW, Clairbois HE, Daffertshofer A, Verbunt J, van Dijk BW, Beek PJ.** MEG-compatible force sensor. *J Neurosci Methods* 144: 193–196, 2005.

6. **Boonstra TW, Daffertshofer A, Roerdink M, Flipse I, Groenewoud K, Beek PJ.** Bilateral motor unit synchronization of leg muscles during a simple dynamic balance task. *Eur J Neurosci* 29: 613–622, 2009.

7. **Boonstra TW, Daffertshofer A, van Ditshuizen JC, van den Heuvel MR, Hofman C, Willigenburg NW, Beek PJ.** Fatigue-related changes in motor-unit synchronization of quadriceps muscles within and across legs. *J Electromyogr Kinesiol* 18: 717–731, 2008.

8. **Campfens SF, Schouten AC, van Putten MJ, van der Kooij H.** Quantifying connectivity via efferent and afferent pathways in motor control using coherence measures and joint position perturbations. *Exp Brain Res* 228: 141–153, 2013.

9. **Chakarov V, Naranjo JR, Schulte-Monting J, Omlor W, Huethe F, Kristeva R.** Beta-range EEG-EMG coherence with isometric compensation for increasing modulated low-level forces. *J Neurophysiol* 102: 1115–1120, 2009.

10. **Conway BA, Halliday DM, Farmer SF, Shahani U, Maas P, Weir AI, Rosenberg JR.** Synchronization between motor cortex and spinal motorneuronal pool during the performance of a maintained motor task in man. *J Physiol* 489: 917–924, 1995.

11. **Daffertshofer A, Lamoth CJ, Meijer OG, Beek PJ.** PCA in studying coordination and variability: a tutorial. *Clin Biomech (Bristol, Avon)* 19: 415–428, 2004.

12. **Danna-Dos Santos A, Poston B, Jesunathadas M, Bobich LR, Hamm TM, Santello M.** Influence of fatigue on hand muscle coordination and EMG-EMG coherence during three-digit grasping. *J Neurophysiol* 104: 3576–3587, 2010.

13. **Efron B, Tibshirani R.** Bootstrap methods for standard errors, confidence intervals, and other measures of statistical accuracy. *Stat Sci* 1: 54–75, 1986.

14. **Engel AK, Fries P.** Beta-band oscillations—signalling the status quo? *Curr Opin Neurobiol* 20: 156–165, 2010.

15. **Evans CM, Baker SN.** Task-dependent intermanual coupling of 8-Hz discontinuities during slow finger movements. *Eur J Neurosci* 18: 453–456, 2003.

16. **Farina D, Holobar A, Merletti R, Enoka RM.** Decoding the neural drive to muscles from the surface electromyogram. *Clin Neurophysiol* 121: 1616–1623, 2010.

17. **Farina D, Merletti R, Enoka RM.** The extraction of neural strategies from the surface EMG. *J Appl Physiol* 96: 1486–1495, 2004.

18. **Farina D, Negro F.** Accessing the neural drive to muscle and translation to neurorehabilitation technologies. *IEEE Rev Biomed Eng* 5: 3–14, 2012.

19. **Farina D, Negro F, Jiang N.** Identification of common synaptic inputs to motor neurons from the rectified electromyogram. *J Physiol* 591: 2403–2418, 2013.

20. **Farmer SF, Bremner FD, Halliday DM, Rosenberg JR, Stephens JA.** The frequency content of common synaptic inputs to motoneurones studied during voluntary isometric contraction in man. *J Physiol* 470: 127–155, 1993.

21. **Farmer SF, Harrison LM, Mayston MJ, Parekh A, James LM, Stephens JA.** Abnormal cortex-muscle interactions in subjects with X-linked Kallmann's syndrome and mirror movements. *Brain* 127: 385–397, 2004.

22. **Farmer SF, Sheean GL, Mayston MJ, Rothwell JC, Marsden CD, Conway BA, Halliday DM, Rosenberg JR, Stephens JA.** Abnormal motor unit synchronization of antagonist muscles underlies pathological co-contraction in upper limb dystonia. *Brain* 121: 801–814, 1998.

23. **Gilbertson T, Lalo E, Doyle L, Di Lazzaro V, Cioni B, Brown P.** Existing motor state is favored at the expense of new movement during 13–35 Hz oscillatory synchrony in the human corticospinal system. *J Neurosci* 25: 7771–7779, 2005.

24. **Grosse P, Brown P.** Acoustic startle evokes bilaterally synchronous oscillatory EMG activity in the healthy human. *J Neurophysiol* 90: 1654–1661, 2003.

25. **Hämäläinen M, Hari R, Ilmoniemi RJ, Knuutila J, Lounasmaa OV.** Magnetoencephalography-theory, instrumentation, and applications to noninvasive studies of the working human brain. *Rev Mod Phys* 65: 413–497, 1993.

26. **Heitmann S, Boonstra TW, Breakspear M.** A dendritic mechanism for decoding traveling waves: principles and applications to motor cortex. *PLoS Comput Biol* 9: e1003260, 2013.

27. **Hellwig B, Schelter B, Guschlbauer B, Timmer J, Lucking CH.** Dynamic synchronisation of central oscillators in essential tremor. *Clin Neurophysiol* 114: 1462–1467, 2003.

28. **Heroux ME, Gandevia SC.** Human muscle fatigue, eccentric damage and coherence in the EMG. *Acta Physiol (Oxf)* 208: 294–295, 2013.

29. **Hurtado JM, Rubchinsky LL, Sigvardt KA.** Statistical method for detection of phase-locking episodes in neural oscillations. *J Neurophysiol* 91: 1883–1898, 2004.

30. **Johnson AN, Shinohara M.** Corticomuscular coherence with and without additional task in the elderly. *J Appl Physiol* 112: 970–981, 2012.

31. **Kantz H, Schreiber T.** *Nonlinear Time Series Analysis.* Cambridge, UK: Cambridge University Press, 2004.

32. **Keenan KG, Farina D, Maluf KS, Merletti R, Enoka RM.** Influence of amplitude cancellation on the simulated surface electromyogram. *J Appl Physiol* 98: 120–131, 2005.

33. **Keenan KG, Massey WV, Walters TJ, Collins JD.** Sensitivity of EMG-EMG coherence to detect the common oscillatory drive to hand muscles in young and older adults. *J Neurophysiol* 107: 2866–2875, 2012.

34. **Kilner JM, Baker SN, Salenius S, Hari R, Lemon RN.** Human cortical muscle coherence is directly related to specific motor parameters. *J Neurosci* 20: 8838–8845, 2000.

35. **Koster B, Lauk M, Timmer J, Poersch M, Guschlbauer B, Deuschl G, Lucking CH.** Involvement of cranial muscles and high intermuscular coherence in orthostatic tremor. *Ann Neurol* 45: 384–388, 1999.

36. **Lundbye-Jensen J, Nielsen JB.** Central nervous adaptations following 1 wk of wrist and hand immobilization. *J Appl Physiol* 105: 139–151, 2008.

37. **Matsuya R, Ushiyama J, Ushiba J.** Prolonged reaction time during episodes of elevated β-band corticomuscular coupling and associated oscillatory muscle activity. *J Appl Physiol* 114: 896–904, 2013.

38. **McClelland VM, Cvetkovic Z, Mills KR.** Rectification of the EMG is an unnecessary and inappropriate step in the calculation of corticomuscular coherence. *J Neurosci Methods* 205: 190–201, 2012.

39. **Mendez-Balbuena I, Huethe F, Schulte-Monting J, Leonhart R, Manjarrez E, Kristeva R.** Corticomuscular coherence reflects interindividual differences in the state of the corticomuscular network during low-level static and dynamic forces. *Cereb Cortex* 22: 628–638, 2012.

40. **Mima T, Hallett M.** Corticomuscular coherence: a review. *J Clin Neurophysiol* 16: 501–511, 1999.

41. **Muthuraman M, Hellriegel H, Paschen S, Hofschulte F, Reese R, Volkmann J, Witt K, Deuschl G, Raethjen J.** The central oscillatory network of orthostatic tremor. *Mov Disord* 28: 1424–1430, 2013.

42. **Myers LJ, Lowery M, O'Malley M, Vaughan CL, Heneghan C, St Clair Gibson A, Harley YX, Sreenivasan R.** Rectification and non-linear pre-processing of EMG signals for cortico-muscular analysis. *J Neurosci Methods* 124: 157–165, 2003.

43. **Negro F, Farina D.** Linear transmission of cortical oscillations to the neural drive to muscles is mediated by common projections to populations of motoneurons in humans. *J Physiol* 589: 629–637, 2011.

44. **Neto OP, Christou EA.** Rectification of the EMG signal impairs the identification of oscillatory input to the muscle. *J Neurophysiol* 103: 1093–1103, 2010.

45. **Nunez PL, Srinivasan R, Westdorp AF, Wijesinghe RS, Tucker DM, Silberstein RB, Cadusch PJ.** EEG coherency. I: Statistics, reference electrode, volume conduction, Laplacians, cortical imaging, and interpretation at multiple scales. *Electroencephalogr Clin Neurophysiol* 103: 499–515, 1997.

46. **Pohja M, Salenius S, Hari R.** Reproducibility of cortex-muscle coherence. *Neuroimage* 26: 764–770, 2005.

47. **Salenius S, Portin K, Kajola M, Salmelin R, Hari R.** Cortical control of human motoneuron firing during isometric contraction. *J Neurophysiol* 77: 3401–3405, 1997.

48. **Schnitzler A, Gross J.** Normal and pathological oscillatory communication in the brain. *Nat Rev Neurosci* 6: 285–296, 2005.

49. **Semmler JG, Ebert SA, Amarasena J.** Eccentric muscle damage increases intermuscular coherence during a fatiguing isometric contraction. *Acta Physiol (Oxf)* 208: 362–375, 2013.

50. **Staudenmann D, Kingma I, Daffertshofer A, Stegeman DF, van Dieen JH.** Improving EMG-based muscle force estimation by using a high-density EMG grid and principal component analysis. *IEEE Trans Biomed Eng* 53: 712–719, 2006.

51. **Staudenmann D, Roeleveld K, Stegeman DF, van Dieen JH.** Methodological aspects of SEMG recordings for force estimation—a tutorial and review. *J Electromyogr Kinesiol* 20: 375–387, 2010.

52. **Stegeman DF, van de Ven WJ, van Elswijk GA, Oostenveld R, Kleine BU.** The alpha-motoneuron pool as transmitter of rhythmicities in cortical motor drive. *Clin Neurophysiol* 121: 1633–1642, 2010.

53. **Taulu S, Kajola M, Simola J.** Suppression of interference and artifacts by the Signal Space Separation Method. *Brain Topogr* 16: 269–275, 2004.

54. **Timmermann L, Gross J, Dirks M, Volkmann J, Freund HJ, Schnitzler A.** The cerebral oscillatory network of Parkinsonian resting tremor. *Brain* 126: 199–212, 2003.

55. **van Wijk BC, Beek PJ, Daffertshofer A.** Differential modulations of ipsilateral and contralateral beta (de)synchronization during unimanual force production. *Eur J Neurosci* 36: 2088–2097, 2012.

56. **van Wijk BC, Beek PJ, Daffertshofer A.** Neural synchrony within the motor system: what have we learned so far? *Front Hum Neurosci* 6: 252, 2012.

57. **Ward NJ, Farmer SF, Berthouze L, Halliday DM.** Rectification of EMG in low force contractions improves detection of motor unit coherence in the β-frequency band. *J Neurophysiol* 110: 1744–1750, 2013.

58. **Williams ER, Baker SN.** Renshaw cell recurrent inhibition improves physiological tremor by reducing corticomuscular coupling at 10 Hz. *J Neurosci* 29: 6616–6624, 2009.

59. **Williams ER, Soteropoulos DS, Baker SN.** Spinal interneuron circuits reduce approximately 10-Hz movement discontinuities by phase cancellation. *Proc Natl Acad Sci USA* 107: 11098–11103, 2010.

60. **Witham CL, Wang M, Baker SN.** Corticomuscular coherence between motor cortex, somatosensory areas and forearm muscles in the monkey. *Front Syst Neurosci* 4: pii: 38, 2010.

61. **Yao B, Salenius S, Yue GH, Brown RW, Liu JZ.** Effects of surface EMG rectification on power and coherence analyses: an EEG and MEG study. *J Neurosci Methods* 159: 215–223, 2007.